Supporting Information

Martin-Sanchez et al. 10.1073/pnas.1716578115

SI Materials and Methods

Reagents. The concentrations of the cytokine mixture were 100 ng/mL TWEAK, 30 ng/mL TNFα, and 30 units/mL IFN-γ (TTI), based on prior experience (1). Benzyloxycarbonyl-Val-Ala-DL-Asp-fluoromethylketone (zVAD-fmk) (BD Bioscience), Nec-1, and Nec-1s (Sigma) were dissolved in DMSO and added 1 h before stimuli. The concentration of zVAD-fmk (25 μM) was based on prior experience and dose–response studies performed in the laboratory and shown to protect MCT cells from apoptosis-inducing stimuli (1). The concentration of the specific RIPK1 kinase activity inhibitors, Nec-1 (30 μM) and necrostatin-1s (Nec-1s, 30 μM) was based on a previous report (2). The RIPK3 inhibitor GSK872 was used at 1 μM. The specific caspase inhibitors IETD and DEVD (caspase 8 and caspase 3, respectively) (R&D Systems) were used at 25–200 μM.

Assessment of Cell Death. Cell viability was estimated using the 3-[4,5-dimethylthiazol-2-yI]-2,5 diphenyltetrazolium bromide (MTT) (Sigma) colorimetric assay. Following stimulation, culture medium was removed and cells were incubated with 1 mg/mL MTT in PBS for 1 h at 37 °C. The resulting formazan crystals were dried and dissolved in DMSO. Absorbance (indicative of cell viability) was measured at 570 nm.

To assess hypodiploid cells, 10,000 cells were seeded in 12-well plates (Costar). Following stimulation, adherent cells were pooled with spontaneously detached cells and incubated in 100 μg/mL propidium iodide (PI), 0.05% Nonidet P-40, and 10 μg/mL RNase A in PBS at 4 °C for >1 h. This assay permeabilizes the cells; thus PI stains both live and dead cells. The percentage of hypodiploid cells was counted by flow cytometry using a FACS Canto Cytometer and FACS Diva Software (BD Biosciences) (3).

For assessment of cell death by annexin V/7-amino-actinomycin D (7-AAD) staining, 5×10^5 cells were washed with ice-cold PBS, diluted in 100 μL binding buffer, and stained with 2.5 μL PE-annexin V and 5 μL 7-AAD. Cells were incubated for 15 min at 37 °C in the dark. Then, 400 μL binding buffer was added just before flow cytometry. Cells were analyzed using a FACS Canto Cytometer and FACS Diva Software (BD Biosciences). Early and late cell death was evaluated on PE fluorescence (annexin V) versus PerCP (7-AAD) plots. Cells stained only with annexin V were evaluated as positive for phosphatidylserine; cells stained with both annexin V and 7-AAD were evaluated as necrotic as defined by the loss of plasma membrane integrity.

Clonogenic Assays. Cells were plated and pretreated with Nec-1 for 1 h and then stimulated with TTI or TTI/zVAD. After 24 h, cells were treated with 50 μM Nec-1 and/or 20 μM sorafenib for 24 h. After 24 h, they were detached with trypsin-EDTA, seeded in Petri dishes, and cultured in 10% FBS-RPMI for 7 d. They were fixed and stained with crystal violet (4). Petri dishes were photographed and cells were resuspended in ethanol:sodium citrate 1:1 (0.1 M, pH 4.2), and absorbance (indicative of colony formation) was measured at 570 nm.

Mitochondrial Membrane Potential. Changes in MMP were determined as differences in tetramethylrhodamine methyl ester (TMRM) fluorescence (Molecular Probes, Thermo Fisher). Adherent cells were pooled with spontaneously detached cells and stained with 150 nM TMRM for 10 min at 37 °C. Fluorescence intensity was measured by flow cytometry using a FACS Canto Cytometer and FACS Diva Software (BD Biosciences). Decreased TMRM fluorescence indicates reduced MMP.

Caspase-3 Activity and Caspase-3 Cleavage. Caspase-3 activity was measured following the manufacturer's instructions (MBL) (1). In brief, cell extracts (70 μg protein) were incubated with 200 μM DEVD-pNA, and pNA light emission was quantified. Comparing the pNA absorbance of an apoptotic sample with a control allows determination of the fold increase in caspase activity. Caspase-3 cleavage was assessed by Western blot using a cleavage-specific antibody (Cell Signaling) and by immunohistochemistry by using another cleavage-specific antibody (Promega), as described below. Caspase-3 cleavage was interpreted as an apoptotic signal with the restriction of possible gasdermin E-mediated necrotic cell death that was recently described (5).

Immunofluorescence. Cells plated onto Labtek slides were fixed in 4% paraformaldehyde and permeabilized in 0.2% Triton X-100/PBS, washed in PBS, and incubated with anti-caspase 3 (1:50; Cell Signaling) followed by Alexa 488-conjugated secondary antibody, respectively (1:300; Invitrogen) (3). Nuclei were counterstained with DAPI.

Immunohistochemistry. Immunohistochemistry was carried out in paraffin-embedded tissue sections of 5 μm thick. The slides were deparaffinized with xylene and graded concentrations of ethanol and then rehydrated. Endogenous peroxidase was blocked by incubation in 3% H_2O_2/methanol (1:1) at 25 °C for 30 min. To assay active caspase 3, the slides were subsequently incubated in PBS with 4% BSA and 6% horse serum, for 1 h at 37 °C to reduce nonspecific background staining, and then incubated overnight at 4 °C with anti-cleaved caspase 3 (1:500; Promega) in PBS containing 4% BSA and 1% serum. To assay PCNA staining, the slides were subsequently incubated in PBS with 1.5% horse serum for 1 h at 37 °C to reduce nonspecific background staining and then incubated overnight at 4 °C with anti-PCNA antibody (1:150; Santa Cruz) in PBS containing 1.5% serum. After being washed with PBS, the sections were incubated with a secondary anti-IgG HRP-conjugated antibody diluted 1:200 in 4% BSA/PBS for 1 h for Fn14 and in 1.5% horse serum/PBS for 1 h for PCNA, washed, and stained with DAB (Dako Diagnostics). Sections were counterstained with Carazzi's hematoxylin. Negative controls included incubation with isotype IgG.

The total number of PCNA positive nuclei was quantitated in 10 randomly chosen fields (20×) per kidney using Image Pro Plus Software (Media Cybernetics). Cleaved caspase-3 staining was evaluated by a quantitative scoring system with the same software in 10 randomly chosen fields (20×) per kidney (6).

Immunofluorescence of tissue sections was performed using the Tyramide SuperBoost Kits with Alexa Fluor tyramides, as recommended by the manufacturer (Invitrogen). Anti-MLKL antibody was used (1:300; Biorbyt) and nuclei were counterstained with DAPI. Images were obtained using a confocal fluorescence microscope (Leica TCS SP5 II) and the imaging software "LAS AF" (Leica).

Tubular injury was evaluated in periodic acid-Schiff (PAS) section by a pathologist (P.C.-O.) who was blinded to the nature of the samples. Evidence of cell injury (loss of brush border, vacuolization), cell desquamation, and tubular dilation and signs of regeneration were scored on a semiquantitative 0–3 scale, and results from each item were added to yield the tubular injury score, which had a maximal value of 5 (7).

siRNA Transfection. Cells were seeded in six-well plates and transfected on the following day with 20 nM scrambled siRNA or

siRNA against RIPK3, RIPK1, or MLKL (Invitrogen) by using lipofectamine (Invitrogen, Thermo Fisher) (3). After 24 h for MLKL and RIPK1 or 48 h for RIPK3, the transfected cells were stimulated.

TUNEL Staining. Terminal deoxynucleotidyl transferase-mediated dUTP nick end labeling (TUNEL) assay was performed in 3-μm-thick sections of paraffin-embedded tissue with the In Situ Cell Death Detection Kit, Fluorescein (Roche Applied Science), according to the manufacturer's instructions.

RNA Extraction and Real-Time PCR. Total RNA was extracted by the TRI Reagent method (Invitrogen) and 1 μg RNA was reverse transcribed with a High Capacity cDNA Archive Kit (Applied Biosystems). Quantitative PCR was performed in a 7500 Real-Time PCR System with the Prism 7000 System SDS Software using predeveloped primers (Applied Biosystems) and RNA expression of different genes was corrected for GAPDH (8).

Western Blotting. Cell samples were homogenized in lysis buffer (50 mM Tris·HCl, 150 mM NaCl, 2 mM EDTA, 2 mM EGTA, 0.2% Triton X-100, 0.3% Nonidet P-40, 0.1 mM PMSF, and 1 μg/mL pepstatin A) then separated by 10% SDS/PAGE under reducing conditions. After electrophoresis, samples were transferred to PVDF membranes (Millipore), blocked with 5% skimmed milk in PBS/0.5% vol/vol Tween 20 for 1 h, washed with PBS/Tween, and incubated with anti-RIPK1 (1:500; BD), anti-MLKL (1:1,000, ab196436; Abcam), anti-mouse phospho-MLKL (1:500; Abcam), anti-cleaved PARP (1:500; Abcam), anti-RIPK3 (1:500; Novus), anti-cleaved caspase 8 (1:1,000; Cell Signaling), and anti-cleaved caspase 3 (1:1,000; Cell Signaling) diluted in 5% milk PBS/Tween. Blots were washed with PBS/Tween and incubated with appropriate horseradish peroxidase-conjugated secondary antibody (1:5,000; GE Healthcare). Blots were developed with the chemiluminescence method (ECL) (Fisher Scientific) and probed with mouse monoclonal anti–α-tubulin antibody (1:10,000; Sigma) or anti-GAPDH (1:5,000; Millipore). Levels of expression were corrected for minor differences in loading.

Isolation of membrane proteins was performed using the Plasma Membrane Protein Extraction Kit (Abcam) following manufacturer's instructions. Na/K-ATPase was used as control of membrane extraction (1:2,500; Cell Signaling) (9).

1. Justo P, et al. (2006) Cytokine cooperation in renal tubular cell injury: The role of TWEAK. *Kidney Int* 70:1750–1758.
2. Linkermann A, et al. (2012) Rip1 (receptor-interacting protein kinase 1) mediates necroptosis and contributes to renal ischemia/reperfusion injury. *Kidney Int* 81:751–761.
3. Martin-Sanchez D, et al. (2017) Deferasirox-induced iron depletion promotes BclxL downregulation and death of proximal tubular cells. *Sci Rep* 7:41510.
4. Lorz C, Justo P, Sanz AB, Egido J, Ortíz A (2005) Role of Bcl-xL in paracetamol-induced tubular epithelial cell death. *Kidney Int* 67:592–601.
5. Wang Y, et al. (2017) Chemotherapy drugs induce pyroptosis through caspase-3 cleavage of a gasdermin. *Nature* 547:99–103.
6. Sanz AB, et al. (2009) Tweak induces proliferation in renal tubular epithelium: A role in uninephrectomy induced renal hyperplasia. *J Cell Mol Med* 13:3329–3342.
7. Martin-Sanchez D, et al. (2017) Ferroptosis, but not necroptosis, is important in nephrotoxic folic acid-induced AKI. *J Am Soc Nephrol* 28:218–229.
8. Sanz AB, et al. (2008) The cytokine TWEAK modulates renal tubulointerstitial inflammation. *J Am Soc Nephrol* 19:695–703.
9. Günther C, et al. (2016) The pseudokinase MLKL mediates programmed hepatocellular necrosis independently of RIPK3 during hepatitis. *J Clin Invest* 126:4346–4360.

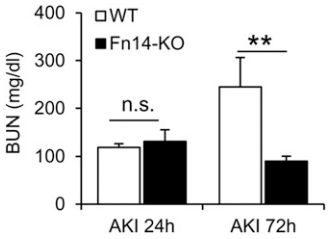

Fig. S1. Fn14 deficiency preserves renal function and reduces cell death in folic acid-induced AKI. AKI was induced by a folic acid overdose in WT and Fn14-KO mice. Mice were killed at 24 and 72 h. Renal function was assessed by BUN levels. Data are expressed as mean ± SEM of n = 7 mice per group. $^{**}P < 0.01$. n.s., nonsignificant.

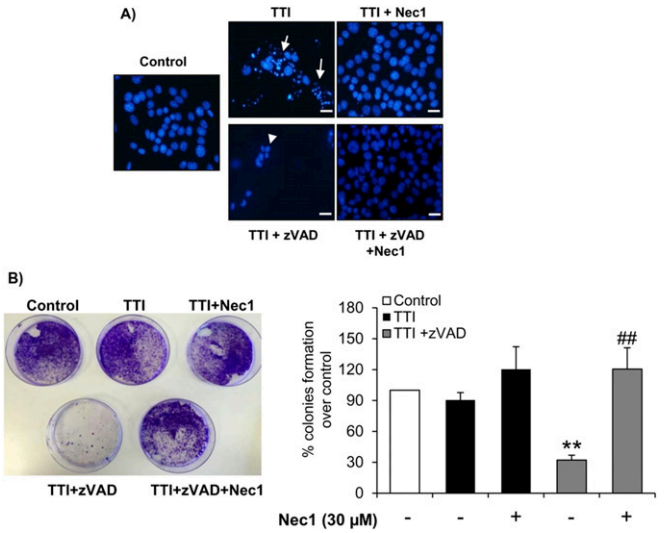

Fig. S2. Nec-1 prevents cell death induced by TWEAK/TNFα/IFNγ (TTI) in cultured tubular cells. Cultured tubular cells were pretreated with zVAD (25 μM) and/or Nec-1 (30 μM) for 1 h and subsequently stimulated with TTI for 24 h. (*A*) Representative photographs of DAPI staining. Fluorescence microscopy, ×400. (Scale bars: 50 μm.) (*B*) Nec-1 preserves long-term survival of TTI/zVAD-treated tubular cells. After treatment, cells were trypsinized, washed, seeded in Petri dishes, and allowed to grow for 7 d; they were stained with crystal violet. For quantification, the colonies were resuspended and absorbance was measured. Nec-1 increased the number of long-term surviving colonies in cells treated with TTI/zVAD. Mean ± SEM of three independent experiments. $^{**}P < 0.01$ vs. control; $^{\#\#}P < 0.05$ vs. TTI/zVAD.

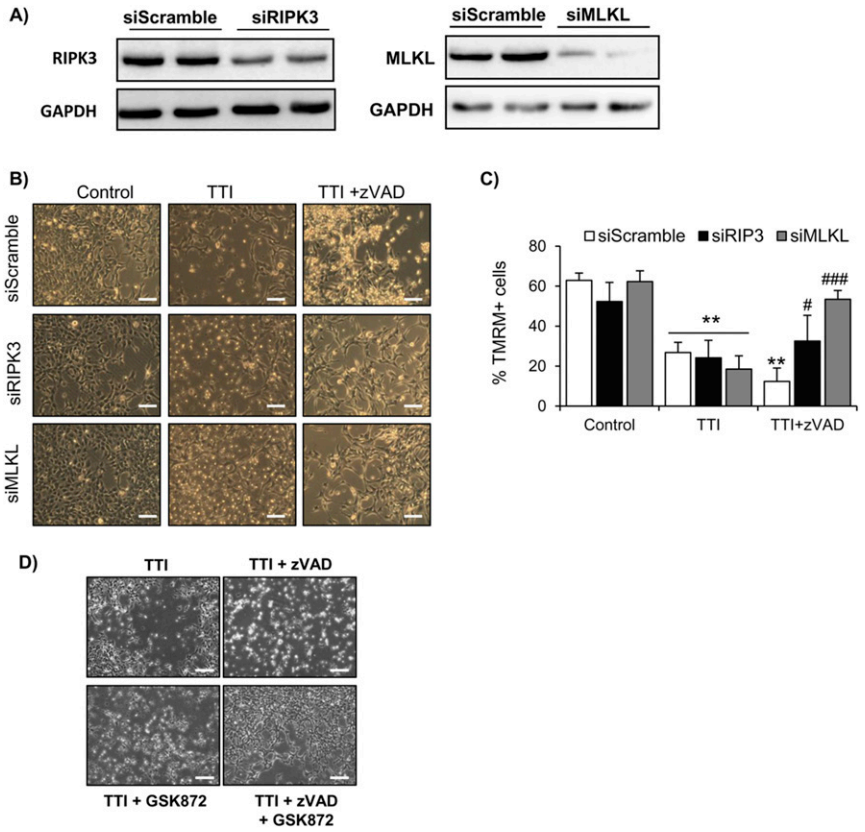

Fig. S3. RIPK3 and MLKL play a key role in TTI/zVAD-induced cell death but not in TTI-induced apoptosis in MCT cells. (*A*) MCT cells were transfected with specific siRNA against RIPK3, MLKL, and RIPK1. After 24 h for MLKL and 48 h for RIPK3, the expression of targeted proteins was checked by Western blot. (*B*) Representative contrast phase microscopy photographs of tubular cells transfected with MLKL, RIPK3, or control (Scramble) siRNA and exposed to TTI or TTI/zVAD for 24 h. Original magnification, 200×. (Scale bars: 200 μM.) (*C*) Transfection with siMLKL prevents MMP loss induced by TTI/zVAD but not by TTI in tubular cells. $^{**}P < 0.01$ vs. control; $^{\#}P < 0.05$ vs. TTI/zVAD siScramble; $^{\#\#\#}P < 0.001$ vs. TTI/zVAD siScramble. (*D*) Representative contrast phase microscopy photographs of tubular cells exposed to TTI and TTI/zVAD following pretreatment with 1 μM GSK872. Original magnification, 200×. (Scale bars: 200 μM.)

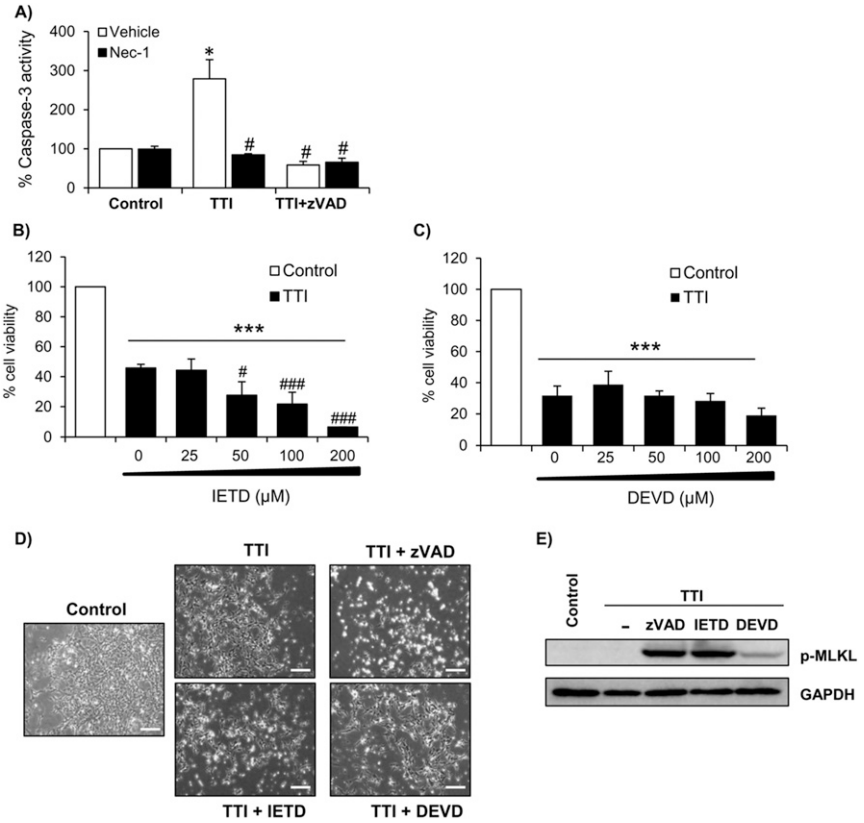

Fig. S4. Nec-1 prevents caspase-3 activation induced by TTI and caspase-8 inhibition increases TTI-induced cell death in cultured tubular cells. (*A*) Nec-1 or zVAD prevents caspase-3 activation induced by TTI for 6 h. Mean ± SEM of three independent experiments. $^{*}P < 0.05$ vs. control; $^{\#}P < 0.05$ vs. TTI. (*B* and *C*) Percentage of tubular cell viability following pretreatment with the caspase-8 inhibitor IETD or the caspase-3 inhibitor DEVD and exposure to TTI for 24 h. Cell viability was assessed by the MTT assay. $^{***}P < 0.001$ vs. control; $^{\#}P < 0.05$ vs. vehicle (0 μM IETD); $^{\#\#\#}P < 0.001$ vs. vehicle (0 μM IETD). (*D*) Representative contrast phase microscopy photographs of tubular cells exposed to TTI for 24 h following pretreatment with vehicle, zVAD (25 μM), and IETD or DEVD (200 μM). Original magnification, 200×. (Scale bars: 200 μM.) (*E*) p-MLKL protein expression in tubular cells exposed to TTI for 6 h following pretreatment with zVAD (25 μM), and IETD or DEVD (200 μM). Representative Western blots of three independent experiments are shown.

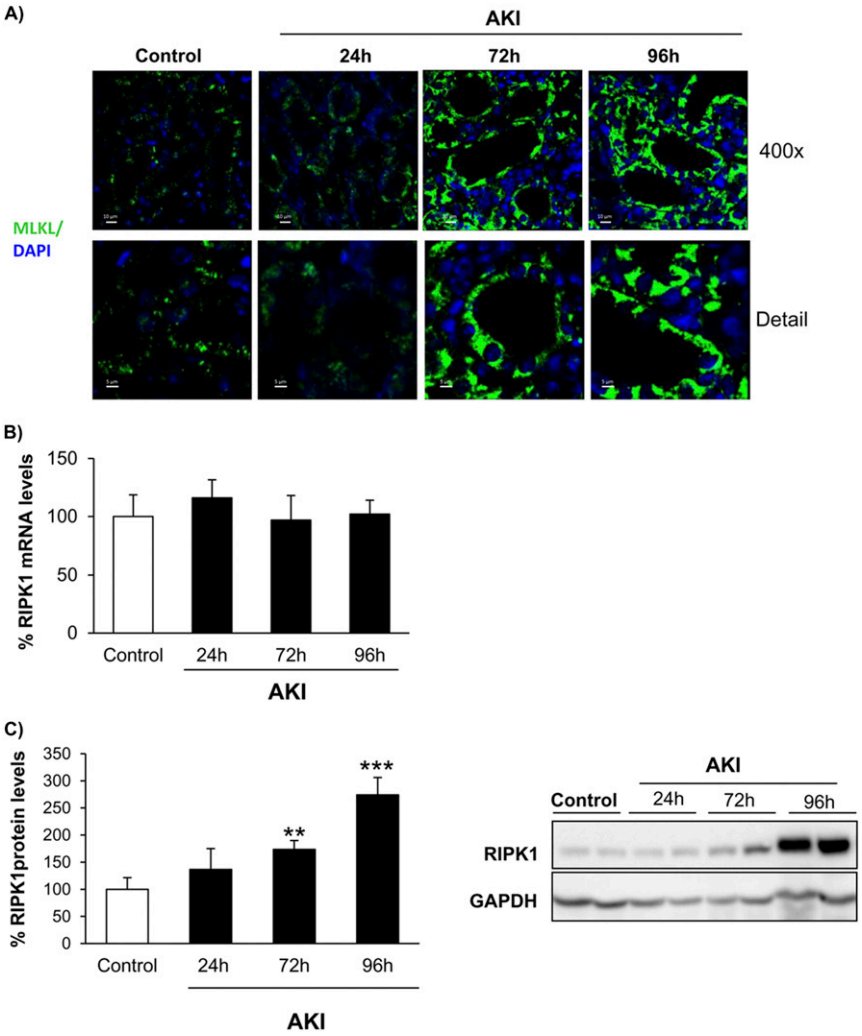

Fig. S5. Time course of necroptotic proteins in AKI. AKI was induced by folic acid overdose. (*A*) Representative images of MLKL localization during AKI. Note increased expression and membrane localization of MLKL at 72 h and 96 h. Confocal microscopy images are shown. (*B* and *C*) Analysis of RIPK1 expression during AKI at the mRNA (*B*) and protein (*C*) levels. Images of representative Western blot. Mean ± SEM of six animals per group. $^{**}P < 0.05$ vs. control; $^{***}P < 0.001$ vs. control.

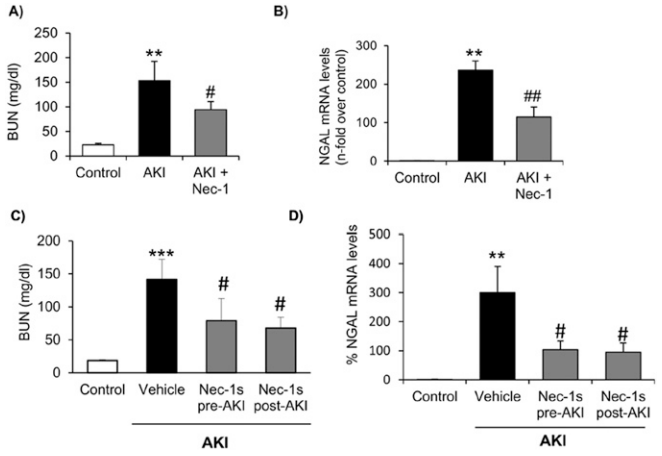

Fig. S6. Nec-1 and Nec-1s functionally prevent folic acid-induced AKI at 96 h in mice. (*A* and *B*) Nec-1 was administered 30 min before induction of folic acid-AKI and then daily until 96 h. (*A*) Renal function assessed by plasma BUN levels. (*B*) NGAL mRNA expression. Data are expressed as mean ± SEM of $n = 10$ mice per group. $^{**}P < 0.01$ vs. control; $^{\#}P < 0.05$ vs. AKI; $^{\#\#}P < 0.01$ vs. AKI. (*C* and *D*) Nec-1s was administered either 30 min before or 6 h after induction of folic acid-AKI and then daily until 96 h. (*C*) Renal function assessed by plasma BUN levels. (*D*) NGAL mRNA expression. Data are expressed as mean ± SEM of $n = 5$ mice per group. $^{**}P < 0.01$ vs. control; $^{***}P < 0.001$ vs. control; $^{\#}P < 0.05$ vs. AKI; $^{\#\#}P < 0.01$ vs. AKI.

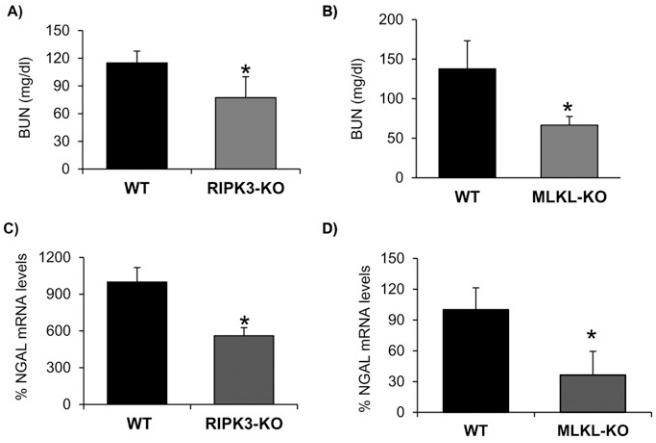

Fig. S7. RIPK3 and MLKL deficiency prevents features of AKI at 96 h. (*A* and *B*) Renal function assessed by plasma creatinine and BUN levels. (*C* and *D*) NGAL mRNA level expression assessed by real-time PCR. Data are expressed as mean ± SEM of $n = 5–10$ mice per group. $*P < 0.05$.

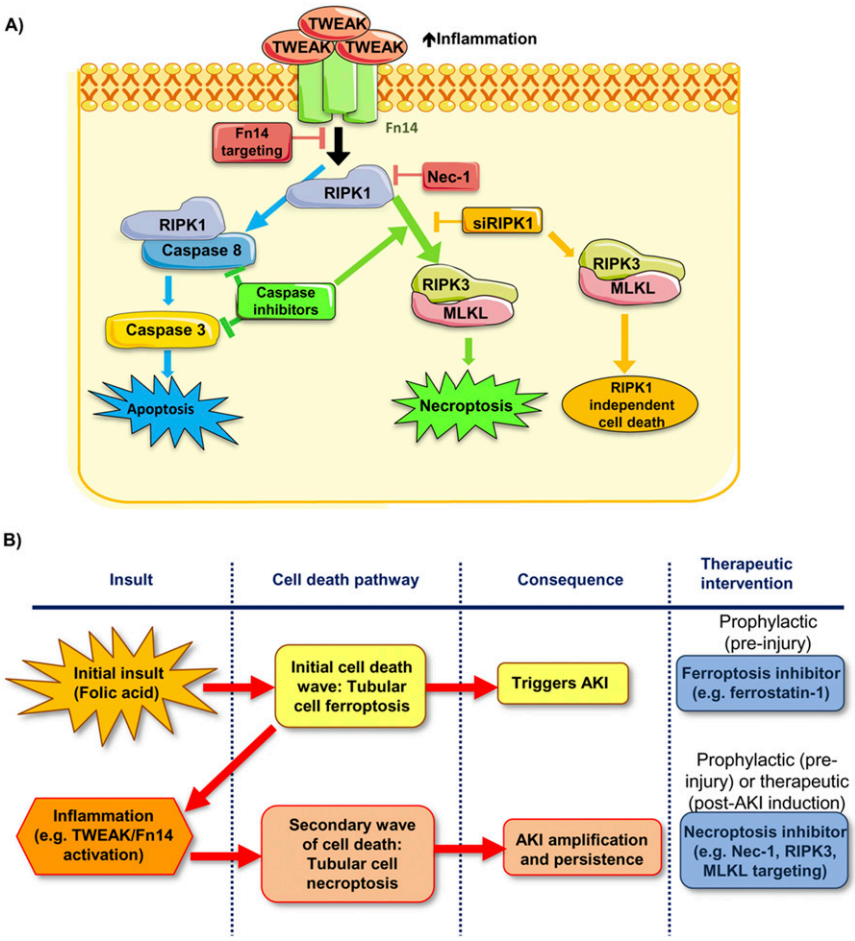

Fig. S8. Schematic summary. (*A*) Cell death signaling induced by TWEAK in a proinflammatory environment. TWEAK in presence of proinflammatory cytokines leads to caspase activation and apoptosis. This may involve the kinase activity of RIPK1. Inhibition of caspase 8 prevents apoptosis, but activates MLKL- and RIPK3-dependent necroptosis. The inhibitor of RIPK1 kinase activity Nec-1 prevented cell death induced by TWEAK, while knockdown of total RIPK1 did not. (*B*) Conceptual sequence of events in toxic AKI and implications for therapy. Integration of data from ref. 5 on ferroptosis and the present manuscript on inflammation and the role of necroptosis in late events are shown.

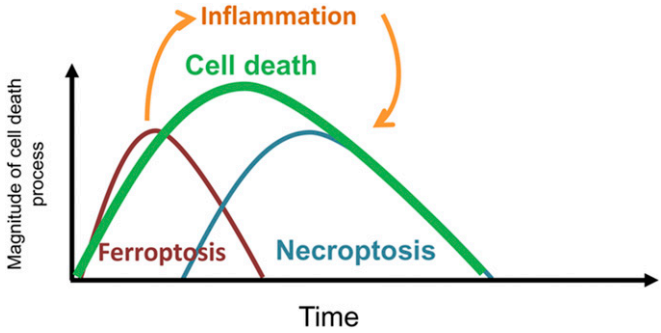

Fig. S9. Contribution of different forms of cell death to AKI, based on present data and those from ref. 3. An initial cell death wave triggered by the original insult is mediated by ferroptosis and triggers a secondary wave of inflammation-dependent necroptotic cell death that amplifies and maintains kidney dysfunction and is sensitive to therapeutic intervention initiated after AKI has been triggered.